Photosensitivity of pulsed laser deposited Ge-Sb-Se thin films

M. Olivier,[1] P. Němec,[1] G. Boudebs,[2] R. Boidin,[1] C. Focsa,[3] and V. Nazabal [1,4,*]

[1]*Department of Graphic Arts and Photophysics, Faculty of Chemical Technology, University of Pardubice, Studentská 573, 53210 Pardubice, Czech Republic*

[2]*LUNAM Université, Université d'Angers, LPhiA, Laboratoire de Photoniques d'Angers, EA 4464, 2 Boulevard Lavoisier, 49045 Angers Cedex 01, France*

[3] *Laboratoire de Physique des Lasers, Atomes et Molécules, Université des Sciences et Technologies de Lille, 59655 Villeneuve d'Ascq, France*

[4]*Institut des sciences chimiques de Rennes, UMR CNRS 6226, Equipe Verres et Céramiques, Université de Rennes 1, 35042 Rennes, France*

**virginie.nazabal@univ-rennes1.fr*

Abstract: Pulsed laser deposition was used to prepare amorphous thin films from $(GeSe_2)_{100-x}$ $(Sb_2Se_3)_x$ system, where x is varying from 0 to 60. Fabricated films present a good morphology with no cracks nor breaks and relatively low roughness. To study their photosensitivity under irradiation with energy close to band gap, a comparison of their optical properties (refractive index and band gap energy) before and after irradiation is performed in both, as-deposited and annealed states. In linear regime, annealed films seem to be photostable when x≥30. In nonlinear regime, highest photoinduced threshold intensity values were found for films with x = 10, 16.7 and x = 30, 40. Thus, the highest photostability in both, linear and nonlinear regimes of irradiation, was observed for layers with x = 30 and 40. Finally, the structure of the films is discussed based on Raman scattering spectroscopy results.

OCIS codes: (350.3390) Laser materials processing; (160.2750) Glass and other amorphous materials; (160.5335) Photosensitive materials; (310.6860) Thin films, optical properties; (300.6450) Spectroscopy, Raman.

References and links

1. C. Meneghini and A. Villeneuve, "As_2S_3 photosensitivity by two-photon absorption: holographic gratings and self-written channel waveguides," J. Opt. Soc. Am. B **15**(12), 2946–2950 (1998).
2. K. Shimakawa, A. Kolobov, and S. R. Elliott, "Photoinduced effects and metastability in amorphous semiconductors and insulators," Adv. Phys. **44**(6), 475–588 (1995).
3. P. Němec, S. Zhang, V. Nazabal, K. Fedus, G. Boudebs, A. Moreac, M. Cathelinaud, and X.-H. Zhang, "Photo-stability of pulsed laser deposited $Ge_xAs_ySe_{100-x-y}$ amorphous thin films," Opt. Express **18**(22), 22944–22957 (2010).
4. A. Zakery and S. R. Elliott, "Optical properties and applications of chalcogenide glasses: a review," J. Non-Cryst. Solids **330**(1-3), 1–12 (2003).
5. M. Olivier, J. C. Tchahame, P. Němec, M. Chauvet, V. Besse, C. Cassagne, G. Boudebs, G. Renversez, R. Boidin, E. Baudet, and V. Nazabal, "Structure, nonlinear properties, and photosensitivity of $(GeSe_2)_{100-x}(Sb_2Se_3)_x$ glasses," Opt. Mater. Express **4**(3), 525 (2014).
6. B. J. Eggleton, B. Luther-Davies, and K. Richardson, "Chalcogenide photonics," Nat. Photonics **5**, 141–148 (2011).
7. M. Frumar, B. Frumarova, P. Nemec, T. Wagner, J. Jedelsky, and M. Hrdlicka, "Thin chalcogenide films prepared by pulsed laser deposition – new amorphous materials applicable in optoelectronics and chemical sensors," J. Non-Cryst. Solids **352**(6-7), 544–561 (2006).
8. S. R. Ovshinsky, "Reversible Electrical Switching Phenomena in Disordered Structures," Phys. Rev. Lett. **21**(20), 1450–1453 (1968).
9. G. Pfeiffer, M. A. Paesler, and S. C. Agarwal, "Reversible photodarkening of amorphous arsenic chalcogens," J. Non-Cryst. Solids **130**(2), 111–143 (1991).

#234197 - $15.00 USD Received 6 Feb 2015; revised 7 Mar 2015; accepted 7 Mar 2015; published 13 Mar 2015

10. K. E. Youden, T. Grevatt, R. W. Eason, H. N. Rutt, R. S. Deol, and G. Wylangowski, "Pulsed laser deposition of Ga-La-S chalcogenide glass thin film optical waveguides," Appl. Phys. Lett. **63**(12), 1601–1603 (1993).
11. V. K. Tikhomirov and S. R. Elliott, "The anisotropic photorefractive effect in bulk As_2S_3 glass induced by polarized subgap laser light," J. Phys. Condens. Matter **7**(8), 1737–1747 (1995).
12. M. Mitkova, M. N. Kozicki, H. C. Kim, and T. L. Alford, "Thermal and photodiffusion of Ag in S-rich Ge–S amorphous films," Thin Solid Films **449**(1-2), 248–253 (2004).
13. L. Calvez, Z. Yang, and P. Lucas, "Light-Induced Matrix Softening of Ge-As-Se Network Glasses," Phys. Rev. Lett. **101**(17), 177402 (2008).
14. A. Kolobov and J. Tominaga, "Chalcogenide glasses in optical recording: recent progress," J. Optoelectron. Adv. Mater. **4**, 679–686 (2002).
15. A. J. Apling, A. J. Leadbetter, and A. C. Wright, "A comparison of the structures of vapour-deposited and bulk arsenic sulphide glasses," J. Non-Cryst. Solids **23**(3), 369–384 (1977).
16. K. Tanaka, "Reversible photostructural change: Mechanisms, properties and applications," J. Non-Cryst. Solids **35–36**(Part 2), 1023–1034 (1980).
17. W. D. Shen, M. Cathelinaud, M. D. Lequime, F. Charpentier, and V. Nazabal, "Light trimming of a narrow bandpass filter based on a photosensitive chalcogenide spacer," Opt. Express **16**(1), 373–383 (2008).
18. M. Chauvet, G. Fanjoux, K. P. Huy, V. Nazabal, F. Charpentier, T. Billeton, G. Boudebs, M. Cathelinaud, and S.-P. Gorza, "Kerr spatial solitons in chalcogenide waveguides," Opt. Lett. **34**(12), 1804–1806 (2009).
19. J. Z. Liu and P. C. Taylor, "Absence of photodarkening in bulk, glassy As_2S_3 and As_2Se_3 alloyed with copper," Phys. Rev. Lett. **59**(17), 1938–1941 (1987).
20. A. Masuda, Y. Yonezawa, A. Morimoto, M. Kumeda, and T. Shimizu, "Influence of Pb incorporation on light-induced phenomena in amorphous $Ge_{100-x-y}Pb_xS_y$ thin films," J. Non-Cryst. Solids **217**(2-3), 121–135 (1997).
21. K. Shimakawa, N. Yoshida, A. Ganjoo, Y. Kuzukawa, and J. Singh, "A model for the photostructural changes in amorphous chalcogenides," Philos. Mag. Lett. **77**(3), 153–158 (1998).
22. E. Vateva, "Giant photo-and thermo-induced effects in chalcogenides," J. Optoelectron. Adv. Mater. **9**, 3108–3114 (2007).
23. E. Sleeckx, L. Tichý, P. Nagels, and R. Callaerts, "Thermally and photo-induced irreversible changes in the optical properties of amorphous Ge_xSe_{100-x} films," J. Non-Cryst. Solids **198–200**(Part 2), 723–727 (1996).
24. M. Frumar, B. Frumarová, T. Wágner, and P. Němec, "Photo-Induced Phenomena in Amorphous and Glassy Chalcogenides," in *Photo-Induced Metastability in Amorphous Semiconductors*, A. V. Kolobov, ed. (Wiley-VCH Verlag GmbH, 2003), pp. 23–44.
25. G. Yang, H. Jain, A. Ganjoo, D. Zhao, Y. Xu, H. Zeng, and G. Chen, "A photo-stable chalcogenide glass," Opt. Express **16**(14), 10565–10571 (2008).
26. P. Hawlova, M. Olivier, F. Verger, V. Nazabal, and P. Nemec, "Photosensitivity of pulsed laser deposited $Ge_{20}As_{20}Se_{60}$ and $Ge_{10}As_{30}Se_{60}$ amorphous thin films," Mater. Res. Bull. **48**(10), 3860–3864 (2013).
27. X. Su, R. Wang, B. Luther-Davies, and L. Wang, "The dependence of photosensitivity on composition for thin films of Ge_x As_y Se_{1-x-y} chalcogenide glasses," Appl. Phys. A - Mater. Sci. Process. **113**(3), 575–581 (2013).
28. P. Khan, A. R. Barik, E. M. Vinod, K. S. Sangunni, H. Jain, and K. V. Adarsh, "Coexistence of fast photodarkening and slow photobleaching in $Ge_{19}As_{21}Se_{60}$ thin films," Opt. Express **20**(11), 12416–12421 (2012).
29. Y. Chen, X. Shen, R. Wang, G. Wang, S. Dai, T. Xu, and Q. Nie, "Optical and structural properties of Ge–Sb–Se thin films fabricated by sputtering and thermal evaporation," J. Alloy. Comp. **548**, 155–160 (2013).
30. V. Nazabal, F. Charpentier, J.-L. Adam, P. Němec, H. Lhermite, M.-L. Brandily-Anne, J. Charrier, J.-P. Guin, and A. Moréac, "Sputtering and Pulsed Laser Deposition for Near- and Mid-Infrared Applications: A Comparative Study of $Ge_{25}Sb_{10}S_{65}$ and $Ge_{25}Sb_{10}Se_{65}$ Amorphous Thin Films," Int. J. Appl. Ceram. Technol. **8**(5), 990–1000 (2011).
31. F. Verger, V. Nazabal, F. Colas, P. Němec, C. Cardinaud, E. Baudet, R. Chahal, E. Rinnert, K. Boukerma, I. Peron, S. Deputier, M. Guilloux-Viry, J. P. Guin, H. Lhermite, A. Moreac, C. Compère, and B. Bureau, "RF sputtered amorphous chalcogenide thin films for surface enhanced infrared absorption spectroscopy," Opt. Mater. Express **3**(12), 2112–2131 (2013).
32. J. Tauc, "Absorption edge and internal electric fields in amorphous semiconductors," Mater. Res. Bull. **5**(8), 721–729 (1970).
33. P. Němec, V. Nazabal, and M. Frumar, "Photoinduced phenomena in amorphous As_4Se_3 pulsed laser deposited thin films studied by spectroscopic ellipsometry," J. Appl. Phys. **106**(2), 023509 (2009).
34. A. Ferlauto, G. M. Ferreira, J. M. Pearce, C. R. Wronski, R. W. Collins, X. Deng, and G. Ganguly, "Analytical model for the optical functions of amorphous semiconductors from the near-infrared to ultraviolet: Applications in thin film photovoltaics," J. Appl. Phys. **92**(5), 2424–2436 (2002).
35. G. Cody, "The optical absorption edge of a-Si: H," Semicond. Semimet. **21**, 11–82 (1984).
36. D. P. Bulla, R. P. Wang, A. Prasad, A. V. Rode, S. J. Madden, and B. Luther-Davies, "On the properties and stability of thermally evaporated Ge–As–Se thin films," Appl. Phys. A - Mater. Sci. Process. **96**(3), 615–625 (2009).
37. V. Nazabal, P. Němec, A. M. Jurdyc, S. Zhang, F. Charpentier, H. Lhermite, J. Charrier, J. P. Guin, A. Moreac, M. Frumar, and J.-L. Adam, "Optical waveguide based on amorphous Er^{3+}-doped Ga–Ge–Sb–S(Se) pulsed laser deposited thin films," Thin Solid Films **518**(17), 4941–4947 (2010).

#234197 - $15.00 USD Received 6 Feb 2015; revised 7 Mar 2015; accepted 7 Mar 2015; published 13 Mar 2015

38. R. P. Wang, D.-Y. Choi, A. Rode, S. J. Madden, and B. Luther-Davies, "Rebonding of Se to As and Ge in $Ge_{33}As_{12}Se_{55}$ films upon thermal annealing: Evidence from x-ray photoelectron spectra investigations," J. Appl. Phys. **101**(11), 113517 (2007).
39. A. Ganjoo, G. Chen, and H. Jain, "Photoinduced changes in the local structure of a-$GeSe_2$ by in situ EXAFS," Phys. Chem. Glas. - Eur. J. Glass Sci. Technol. Part B **47**, 177–181 (2006).
40. L. Tichy and H. Ticha, "On the "compositional threshold" in GeS_2-Sb_2S_3, $GeSe_2$-Sb_2Se_3 and GeS_2-Bi_2S_3 glasses," Mater. Chem. Phys. **152**, 1–3 (2015).

1. Introduction

Chalcogenide glasses and amorphous thin films are typically sensitive to light exposure [1–3] and present large nonlinearity [4]. They show high Kerr nonlinearities at femtoseconds time scale and high third order susceptibility $\chi(3)$ which can be up to three orders of magnitude larger than that of silica glass [5]. That is why amorphous chalcogenides have been studied for ultrafast switching in telecommunication systems [6] or for sensing application [7]. Photosensitivity in amorphous chalcogenides, typically under irradiation of light with a wavelength near the band gap [2], is related to a mechanism involving creation of electron-holes pairs, which may change the valence of neighboring atoms and their chemical bonds [8]. Depicted bond switching induced by illumination can result in macroscopic changes of physical properties of the material. Commonly observed photoinduced phenomena involve changes in optical properties, specifically the band gap energy changes (photodarkening (PD) [9] or photobleaching (PB) [10]) or the refractive index modifications (photorefraction [11]). Modifications in other physical properties such as photodiffusion [12], photofluidity [13] and photocrystallization [14] were reported as well. All mentioned effects are observed in bulk materials; however they are particularly pronounced in thin films. One of the reasons is that film can condense into amorphous state with a large number of defective bonds, creating a different topology from that of bulk glasses [15]. Two main types of effects, stimulated by irradiation, may be observed in amorphous chalcogenide thin film depending on whether the film is as-deposited or suitably annealed (relaxed). In the first case, the irreversible effects can occur in as-deposited thin film while a completely stress-free relaxed film will present reversible effects that can be removed by re-annealing [16]. In spite of the fact that photoinduced phenomena can be of interest for applications such as optical writing or photolithography [1,4,17], for applications in the field of infrared optics, involving linear and nonlinear optical properties, amorphous chalcogenide insensitive to light exposure are required [18].

The magnitude of photosensitivity in amorphous chalcogenides might be decreased by adding of some metallic elements, for example Cu, Sn or Pb in small quantity (less than 2-5%, higher for Pb) [19,20]. The models usually proposed for explaining the reversible PD of $As_2S(Se)_3$ thin films highlight the likely broadening of the valence band related to the lone-pair of the chalcogens. Another model, in which the presence of photoexcited charge carriers in extended states leads to an interlayers distance increase and/or a slip along the layers affecting the lone-pair of the chalcogens, was also suggested [21]. In the frame of this model, it was proposed that the disappearance of PD effect may be referred to the formation of bridges between the As_2Se_3 layers caused by metallic elements. The presence of tetrahedrally coordinated chalcogen atoms more than the tetrahedral coordination of the Cu was suggested as a reason leading to the vanishing of PD effect in $As_2S(Se)_3$ glasses containing Cu [19].

In case of as-deposited Ge-based amorphous chalcogenides, an irreversible PB is usually obtained; during the annealing of the as-deposited films, bleaching of the films is observed as well. For relaxed Ge-based films, reversible PD effect is reported [22–24]. In case of Ge-Pb-S thin films, two mechanisms explaining the vanishing of PD were proposed [20]. First mechanism could be connected with the masking of PD via the electronic states originating in Pb incorporation; the energy of such states is higher than energy of states related with photostructural changes. Second mechanism of PD disappearance is associated with an increase in the coordination number of chalcogen atoms. Thus, in case of metal

#234197 - $15.00 USD Received 6 Feb 2015; revised 7 Mar 2015; accepted 7 Mar 2015; published 13 Mar 2015

incorporation, the disappearance of the PD seems to result mainly from the disappearance of the photostructural effects.

However, the optimization studies to find intrinsic composition of amorphous chalcogenides preventing undesired photoinduced effects are rare up to date [3,25].

In our previous work, we showed that some photostable thin films prepared using pulsed laser deposition (PLD) exist in Ge-As-Se system [3,26]. Study recently performed by Su presented photostability of Ge-As-Se thermally evaporated films (after annealing at 80 °C) for mean coordination number (MCN) ~2.45-2.50 [27]. It is worthy to mention also coexistence of fast PD and slow PB in thermally evaporated Ge-As-Se films reported by Khan [28].

The idea of photostability finding in Ge-As-Se system could be based on the assumption of PD and PB effects compensation; PD and PB were observed in binary As and Ge based amorphous chalcogenide thin films, respectively. As a next step, we focus on the photosensitivity/photostability study in Ge-Sb-Se amorphous films. The use of antimony is beneficial regarding its lower toxicity in comparison with arsenic. Further, we depicted nonlinear properties of chalcogenide glasses from $(GeSe_2)_{100-x}(Sb_2Se_3)_x$ system concluding that nonlinear refractive index as well as two photon absorption coefficient increase with increasing content of Sb_2Se_3 [5]. At 1.55 μm in femtosecond regime, photosensitivity of these bulk glasses attributed to two photon absorption is shown to be very dependent on composition. It is noteworthy that for bulk glasses with intermediate Sb_2Se_3 content (at x = 30-40), photosensitivity at 1.55 μm is strongly reduced. The development of integrated optical devices for nonlinear applications based on chalcogenide materials requires the fabrication of chalcogenide thin films presenting a photostable behavior in linear and nonlinear regime. Thus, the aim of this work is to explore photosensitivity/photostability in pseudo-binary $(GeSe_2)_{100-x}(Sb_2Se_3)_x$ thin films in order to confirm suitability of this system for linear and nonlinear optical applications.

It was already shown that Ge-Sb-Se thin films can be fabricated by different deposition techniques such as thermal evaporation [29], radio-frequency (rf) magnetron sputtering [30,31] or PLD [30]. PLD method seems to be favorable according to its simplicity, easy control of the process and often stoichiometric transfer of the material from the target to the film [7].

In this paper, photosensitivity/photostability of selected Ge-Sb-Se amorphous thin films is studied under irradiation with continuous, close to band gap light in both, as-deposited and annealed state. Changes in optical properties of the films are explored regarding influence of the insertion of Sb_2Se_3. Different methods of characterization such as scanning electron microscopy (SEM), energy dispersive spectroscopy (EDS), atomic force microscopy (AFM), Raman scattering spectroscopy, transmittance measurements, variable angle spectroscopic ellipsometry (VASE), and non-linear imaging technique with phase object (NIT-PO) inside the 4f imaging system were employed to have comprehensive picture of fabricated layers.

2. Materials and experimental methods

Targets used for PLD are 25 mm diameter chalcogenide glasses from $(GeSe_2)_{100-x}(Sb_2Se_3)_x$ system, where x is varying from 0 to 60. For a comparison, the commercial composition $Ge_{28}Sb_{12}Se_{60}$ (known as AMTIR-3 or IG5, Schott Inc.) was studied. Chalcogenide glasses were prepared using the conventional melting and quenching vacuum method, from commercial elements (Ge, Sb and Se) of high purity (5N), following our previous work [5].

Thermal characteristics of fabricated bulk glasses were determined by differential scanning calorimeter (DSC, Q20 DSC, TA Instruments). DSC measurements were performed on 10 mg powdered samples, heated up to 450 °C at heating rate of 10 °C.min^{-1}. X-ray diffraction data (XRD) were recorded with a D8-Advance diffractometer (Bruker AXS, Germany) with Bragg–Brentano θ–θ geometry (40 kV, 40 mA) using CuKα radiation with

#234197 - $15.00 USD Received 6 Feb 2015; revised 7 Mar 2015; accepted 7 Mar 2015; published 13 Mar 2015

secondary graphite monochromator. The diffraction angles were measured at room temperature from 5 to 65° (2θ) within 0.02° steps with a counting time of 5 s per step.

Thin films were obtained using PLD. Targets were ablated with a KrF excimer laser emitting at 248 nm. Output pulse energy was 300 ± 3 mJ with pulses duration of 30 ns and repetition rate was 20 Hz. Laser fluency was set at 2.6 J.cm^{-2}. Pressure in the vacuum chamber at the beginning of deposition was about 3-4.10^{-4} Pa. In order to obtain films with uniform thickness, off axis PLD technique with rotating substrates and targets was used. The substrates were positioned parallel to the target at a distance of 5 cm.

Selected thin films deposited on silica/microscope glass substrates were annealed, under inert Ar atmosphere, during 2 hours at a temperature 30 K below the glass transition temperature of the corresponding bulk glass. The samples were then slowly cooled down to room temperature (1 K.min^{-1}).

Study of reversible and irreversible photoinduced phenomena in linear regime was carried out with as-deposited and annealed thin films deposited on microscope glass slides. Photosensitivity was studied for exposures (2 hours) with laser light having energy (wavelength) in band gap region, with a power density of 160 mW.cm^{-2} and a laser-sample distance of 100 cm, except for 660 nm laser for which power density and laser-sample distance was 120 mW.cm^{-2} and 20 cm, respectively. To avoid the oxidation of the films during irradiation, the samples were maintained under nitrogen atmosphere. For exposure experiments, 6 different laser wavelengths were available: 532 nm (2.33 eV), 593 nm (2.09 eV), 635 nm (1.95 eV), 660 nm (1.88 eV), 690 nm (1.80 eV) and 808 nm (1.53 eV).

To investigate nonlinear photoinduced effects in annealed chalcogenide thin films, the NIT-PO approach inside the 4f imaging system was used at 1064 nm [3] for layers deposited on SiO_2 substrates. As a result, photosensitivity in nonlinear regime was characterized by photoinduced threshold intensity values I_{0T} (GW.cm^{-2}).

The chemical composition of $(GeSe_2)_{100-x}(Sb_2Se_3)_x$ bulk glasses and corresponding thin films was determined with EDS (JSM 6400, Oxford Link INCA). The morphology of thin films was studied using SEM technique (JEOL JSM 6301F). Films' roughness was estimated with an AFM instrument (Solver-Pro M, NT-MTD).

Transmission spectra of PLD films were obtained in visible and NIR range (500-2000 nm) employing Perkin Elmer Lambda 1050 spectrophotometer. Tauc's approach was used to evaluate the optical band gap of thin films under study [32]. Refractive indices and extinction coefficient spectral dependencies of thin films were extracted from the variable angle spectroscopic ellipsometry data measured with an automatic rotating analyzer ellipsometer (VASE, J. A. Woollam Co., Inc.). Measurements parameters were following: spectral region 300-2300 nm (i.e. 4.13-0.54 eV) with wavelength steps of 10 nm and angles of incidence of 50°, 60°, and 70°. The optical responses of thin $(GeSe_2)_{100-x}(Sb_2Se_3)_x$ films were fitted using the Cody-Lorentz (CL) model, which is appropriate to describe amorphous chalcogenide thin films/amorphous semiconductors optical functions and their photo-induced changes [3,33–35]. Note that thicknesses of thin films, thickness uniformity and thickness of the surface layer (assuming to be composed of thin film material mixed with 50% of voids) were fitting parameters. The VASE experimental data were analyzed using a three layer model: (1) a glassy substrate, (2) an amorphous chalcogenide thin film and (3) a rough surface layer.

To evaluate the structure of fabricated thin films, micro-Raman spectroscopy was used. The Raman spectra were recorded at room temperature under 785 nm excitation, with an InVia reflex spectroscope (Renishaw) coupled to an Olympus BFXM free space x50 microscope.

3. Results and discussion

We successfully prepared homogeneous bulk chalcogenide glasses of compositions detailed in Table 1. The bulk sample containing highest Sb_2Se_3 content (x = 70) presented some

#234197 - $15.00 USD Received 6 Feb 2015; revised 7 Mar 2015; accepted 7 Mar 2015; published 13 Mar 2015

crystals, evidenced by XRD data. This composition is at the border of the glass forming region and it is thus difficult to obtain homogeneous 25 mm diameter glassy targets. No further studies were thus performed with this composition.

Two depositions were performed for each composition: (1) first deposition of ~900-1400 nm films using both, SiO_2 and Si substrates, to determine composition (EDS), to investigate nonlinear photoinduced effects (NIT-PO), to observe morphology (SEM), and to study the effect of annealing on band gap and refractive index, (2) a second deposition using microscope glass substrates to prepare films for photosensitivity experiments with thickness (~150-1100 nm) close to penetration depth of the light used for irradiation.

3.1 Influence of annealing

As-deposited $(GeSe_2)_{100-x}(Sb_2Se_3)_x$ thin layers were homogeneous according to SEM observations [Fig. 1]. The films show a good planarity with a smooth surface and no cracks nor breaks. Only rarely, sub-micrometers size droplets were observed within few samples. AFM scans were performed (7 x 7µm area) and RMS roughness of thin films was typically comprised between 1.5 and 2 nm indicating their acceptable smoothness.

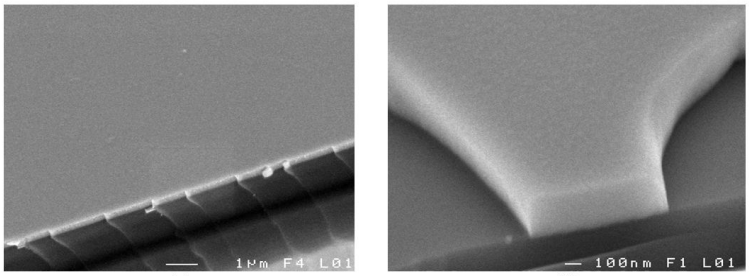

(a) **(b)**

Fig. 1. SEM micrographs of $(GeSe_2)_{60}(Sb_2Se_3)_{40}$ (a) and $(GeSe_2)_{90}(Sb_2Se_3)_{10}$ (b) PLD films.

The chemical composition, as determined by EDS, of both bulk glasses and thin films is listed in Table 1. The films show some loss of selenium in comparison with real targets composition; this loss (lower than 4 at.%) is probably coming from higher volatility of this element compared to germanium and/or antimony. As a result, mean coordination number of the amorphous network is always higher in case of thin films compared to bulk glasses. This phenomenon has already been observed in previous studies [7,30].

The results of VASE data analysis for bulk $(GeSe_2)_{100-x}(Sb_2Se_3)_x$ glasses, as-deposited, and annealed thin films in terms of optical band gap and refractive indices at 1550 nm are presented in Fig. 2. In agreement with the band gap compositional trend for bulk $(GeSe_2)_{100-x}(Sb_2Se_3)_x$ glasses, band gap decreases from ~1.85 to ~1.36 eV for as-deposited films as the content of antimony increases [Fig. 2]. The annealing of the films generally leads to higher values of band gap respecting initial decrease of band gap values (from ~2.11 to ~1.42 eV) with increasing antimony content. Refractive index at 1550 nm increases from ~2.48 to ~3.08 in case of as-deposited films and from ~2.41 to ~3.10 in case of annealed films with rising antimony content. The annealing of Ge-Sb-Se thin films clearly induces an increase in their band gap values as well as a decrease of their refractive indices, reaching values closer to bulk characteristics. Usually, annealing is responsible for structural relaxation of the amorphous network.

We note that in case of studied $(GeSe_2)_{100-x}(Sb_2Se_3)_x$ thin films, the differences between optical characteristics of as-deposited and annealed layers are lower for samples with higher Sb_2Se_3 content. This behavior has already been observed in Ge-As-Se thin films, for which films with lower MCN were not affected by annealing [36]. However, a more complete structural study is needed to fully understand this behavior.

#234197 - $15.00 USD Received 6 Feb 2015; revised 7 Mar 2015; accepted 7 Mar 2015; published 13 Mar 2015

Table 1. Theoretical and real chemical composition of bulk $(GeSe_2)_{100-x}(Sb_2Se_3)_x$ glasses and corresponding PLD thin films (deposited on SiO_2 substrates) estimated by EDS. MCN and MCN* are mean coordination numbers calculated from theoretical and real composition, respectively. Glass transition temperatures (Tg) were evaluated by DSC (± 2 °C). B and F stand for bulk and film, respectively. Thicknesses (d) of thin films were obtained from VASE data analysis (± 5 nm). Last right column contains photoinduced threshold intensity values I_{0T} ($GW.cm^{-2}$) (± 20%).

x	Theoretical composition	MCN	B/F	Tg (°C)	d (nm)	Real composition (± 0.5 at.%)	MCN*	I_{OT}
0	$Ge_{33}Se_{67}$	2.66	B	282	920	$Ge_{36.5}Se_{63.5}$	2.73	
			F			$Ge_{38.7}Se_{61.3}$	2.77	
5	$Ge_{30.6}Sb_{3.2}Se_{66.1}$	2.64	B	358		$Ge_{32.8}Sb_{4.2}Se_{63.0}$	2.65	
			F		1120	$Ge_{32.8}Sb_{4.2}Se_{63.0}$	2.70	15.6
10	$Ge_{28.1}Sb_{6.3}Se_{65.6}$	2.63	B	340		$Ge_{28.3}Sb_{6.8}Se_{64.9}$	2.63	
			F		1120	$Ge_{29.6}Sb_{8.5}Se_{61.8}$	2.68	30.0
16.7	$Ge_{25}Sb_{10}Se_{65}$	2.60	B	308		$Ge_{27.0}Sb_{10.1}Se_{62.8}$	2.64	
			F		1130	$Ge_{26.2}Sb_{12.8}Se_{61.0}$	2.65	29.2
20	$Ge_{23.5}Sb_{11.8}Se_{64.7}$	2.59	B	310		$Ge_{23.1}Sb_{13.0}Se_{63.9}$	2.59	
			F		1400	$Ge_{24.1}Sb_{15.4}Se_{60.5}$	2.64	18.7
30	$Ge_{19.4}Sb_{16.7}Se_{63.9}$	2.56	B	280		$Ge_{19.5}Sb_{17.8}Se_{62.7}$	2.57	
			F		1320	$Ge_{19.2}Sb_{20.9}Se_{59.9}$	2.59	24.7
40	$Ge_{15.8}Sb_{21.1}Se_{63.2}$	2.53	B	271		$Ge_{14.9}Sb_{22.3}Se_{62.8}$	2.52	
			F		1000	$Ge_{15.2}Sb_{25.7}Se_{59.1}$	2.56	32.6
50	$Ge_{12.5}Sb_{25}Se_{62.5}$	2.50	B	250		$Ge_{12.1}Sb_{25.5}Se_{62.5}$	2.50	
			F		1100	$Ge_{12.6}Sb_{26.8}Se_{60.6}$	2.52	18.0
60	$Ge_{9.5}Sb_{28.6}Se_{61.9}$	2.48	B	227		$Ge_{10.4}Sb_{29.1}Se_{60.5}$	2.50	
			F		1210	$Ge_{9.4}Sb_{28.9}Se_{61.7}$	2.53	13.5
IG5	$Ge_{28}Sb_{12}Se_{60}$	2.68	B	285		$Ge_{29.0}Sb_{11.9}Se_{59.1}$	2.70	
			F		1130	$Ge_{28.8}Sb_{15.4}Se_{55.8}$	2.73	11.2

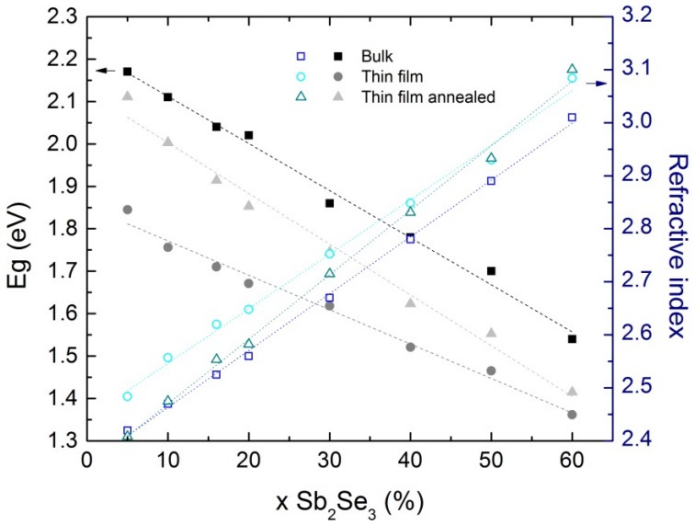

Fig. 2. Optical band gap (± 0.01 eV) and refractive indices (at 1550 nm, ± 0.01) values of bulk $(GeSe_2)_{100-x}(Sb_2Se_3)_x$ glasses, corresponding as-deposited and annealed thin PLD films (with thickness of ~1000-1400 nm) determined from VASE data analysis.

3.2 Influence of irradiation

For the second series of fabricated films, deposited in order to study their behavior under irradiation, their optical characteristics were determined using two different techniques. First, Tauc's plots ($(\alpha h\nu)^{1/2}$ vs. $h\nu$ dependences) were drawn based on transmission data; α stands for the absorption coefficient of thin films (cm^{-1}), ν is the frequency of the light (s^{-1}) and h is

#234197 - $15.00 USD Received 6 Feb 2015; revised 7 Mar 2015; accepted 7 Mar 2015; published 13 Mar 2015

the Planck's constant. Secondly, optical characteristics were extracted from VASE data. Note that both methods of optical band gap determination give results in relatively good agreement. In case of studied materials, the applicability of CL model for the analysis of VASE data is confirmed by low values of mean square errors (typically below 5). Figure 3 represents the evolution of thin films optical properties (obtained by ellipsometry) before and after band gap irradiation. Irradiation energies vary from 1.53 to 2.33 eV and thicknesses of films varied from ~150 to ~1100 nm.

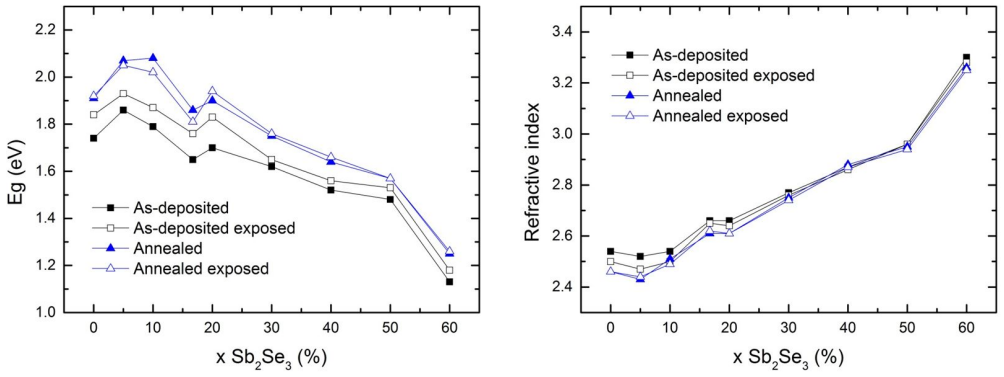

(a) (b)

Fig. 3. Optical parameters of as-deposited, irradiated, annealed and post-annealing irradiated $(GeSe_2)_{100-x}(Sb_2Se_3)_x$ thin films (with thickness of ~150-1100 nm) extracted from VASE data: optical band gap values (a) and refractive indices at 1550 nm (b).

The exposure of $(GeSe_2)_{100-x}(Sb_2Se_3)_x$ as-deposited thin films always induces PB, i.e. an increase of the optical band gap energy. Band gap energy difference between as-deposited and irradiated layers was found to be in range of ~0.02-0.13 eV and ~0.01-0.05 eV according to VASE [Fig. 3(a)] and Tauc's plots results, respectively.

On the other hand, behavior of annealed thin films under irradiation is more complicated. Exposure of annealed thin films results in PD effect, at least for layers with low Sb content, i.e. from x = 5 to 16.7. Here, PD corresponds to a decrease of E_g^{opt}, from –0.02 to –0.06 eV. Contrary, for the films with x = 20, weak PB was found.

Concerning annealed thin films with higher Sb_2Se_3 content (i.e. x>20), no significant change is observed in E_g^{opt} values due to exposure. This analysis is performed based on VASE data and/or Tauc's plots for two irradiation wavelengths. In case of very high Sb content, i.e. for $(GeSe_2)_{40}(Sb_2Se_3)_{60}$ annealed thin films, a slight PD effect is observed, according to Tauc's plots.

Unfortunately, due to uncertainties of band gap and refractive index determination (± 0.01), slight changes cannot be clearly revealed and only tendencies can be highlighted. In term of photostability, the best results were found for annealed $(GeSe_2)_{70}(Sb_2Se_3)_{30}$ layers and generally for films with x>20, having a mean coordination number of ≤2.59. Indeed, films with x>20 are almost insensitive to irradiation in relaxed state. This finding is supporting our previous study within $(GeSe_2)_{100-x}(Sb_2Se_3)_x$ bulk glasses where the photosensitivity attributed to two photon absorption is strongly reduced for glasses with x = 30-40 [5].We note that measured chemical composition of $(GeSe_2)_{70}(Sb_2Se_3)_{30}$ thin films, as determined using EDS (Table 1), is $Ge_{19.2}Sb_{20.9}Se_{59.9.}$ In Ge-As-Se system, $Ge_{20}As_{20}Se_{60}$ (MCN = 2.6) was found to be a photostable composition [3, 26]. Calvez *et al.* [13] mentioned that photostructural changes such as photodarkening decrease and tend to vanish in overcoordinated glasses, i.e. when MCN = 2.6 in Ge-As-Se system. In Ge-Sb-Se system studied here, $(GeSe_2)_{95}(Sb_2Se_3)_5$, $(GeSe_2)_{90}(Sb_2Se_3)_{10}$ and $(GeSe_2)_{83.3}(Sb_2Se_3)_{16.7}$ have MCN higher than 2.6, nevertheless we observed slight PD in annealed state. The films with higher x (having MCN <2.60) present

#234197 - $15.00 USD Received 6 Feb 2015; revised 7 Mar 2015; accepted 7 Mar 2015; published 13 Mar 2015

almost no sensitivity to irradiation in relaxed state leading to the conclusion that the dependence of photosensitivity on MCN is for studied $(GeSe_2)_{100-x}(Sb_2Se_3)_x$ films of different behavior than in Ge-As-Se glasses.

For $Ge_{28}Sb_{12}Se_{60}$ films, slight PD is observed for annealed samples by VASE. However, Tauc's plots indicate stability of band gap values. MCN of $Ge_{28}Sb_{12}Se_{60}$ films is >2.60, thus slight reversible PD is in accordance with results mentioned above.

As-deposited thin films with low Sb content (x≤10) show some decrease in refractive index after exposure (up to −0.05). The films with higher Sb content present almost zero photorefraction in as-deposited state [Fig. 3(b)]. In term of refractive index, relaxed samples are globally more photostable; their photorefraction is found to be close to zero for all the compositions under study.

As observed in case of the first series study, the annealing of Ge-Sb-Se thin films induces a relaxation of the layers resulting in a decrease of their refractive indices, leading to the values closer to parent bulk glasses. This decrease seems to be less important for samples with higher Sb_2Se_3 concentration [Fig. 4].

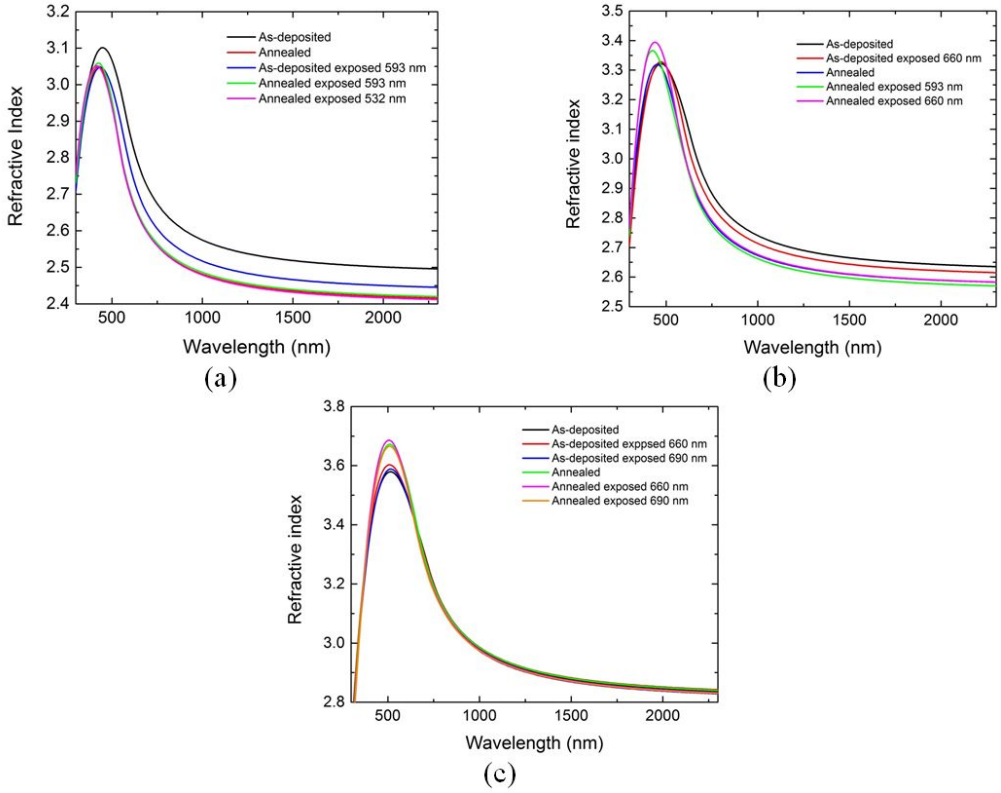

Fig. 4. $(GeSe_2)_{100-x}(Sb_2Se_3)_x$ thin films' refractive index spectral dependencies extracted from VASE data analysis: $(GeSe_2)_{95}(Sb_2Se_3)_5$ (a), $(GeSe_2)_{80}(Sb_2Se_3)_{20}$ (b), and $(GeSe_2)_{60}(Sb_2Se_3)_{40}$ (c).

Looking at presented results, one can conclude that for $(GeSe_2)_{100-x}(Sb_2Se_3)_x$ PLD thin films, where x>20%, annealing/irradiation have low impact on optical parameters of the layers, if any. On the other hand, films with x≤20 present more pronounced changes of optical properties under annealing/irradiation.

Compositional dependence of photosensitivity in nonlinear regime evaluated via photoinduced threshold intensity values I_{0T} (Table 1) is not straightforward; however, highest

#234197 - $15.00 USD Received 6 Feb 2015; revised 7 Mar 2015; accepted 7 Mar 2015; published 13 Mar 2015

photostability was observed for two pairs of layers' composition with x = 10, 16.7 and x = 30, 40.

To look deeper for explanation of observed behavior, the structure of the films was studied by means of Raman scattering spectroscopy.

3.3 Structure of thin films by analysis of Raman scattering spectra

A structural study of $(GeSe_2)_{100-x}(Sb_2Se_3)_x$ bulk glasses using Raman scattering spectroscopy has been previously reported [5]. To summarize, the structure of $(GeSe_2)_{100-x}(Sb_2Se_3)_x$ bulk glasses is basically formed by $[GeSe_{4/2}]$ tetrahedra (connected by corners or edges) and $SbSe_{3/2}$ pyramids. However, a slight presence of homopolar bonds (Se-Se, Ge-Ge, Sb-Sb) was also identified. Introduction of Sb_2Se_3 in the amorphous matrix seems to induce a progressive change in the network, first favoring edge-shared $[Ge_2Se_{8/2}]$ entities. Then, at intermediate Sb_2Se_3 contents, glassy network contains significant number of $SbSe_{3/2}$ pyramids. Finally, at high concentration of Sb in $(GeSe_2)_{100-x}(Sb_2Se_3)_x$ glasses, number of Se_2Sb-$SbSe_2$ structural units seems to appear (increase of homopolar Sb-Sb bonds).

Raman scattering spectra of PLD Ge-Sb-Se thin films have been recorded at all stages. Basically, the quality of Raman spectra is lower for the thin films when compared to bulk glasses. Individual Raman bands are broader due to a larger degree of disorder in thin amorphous films. Raman scattering spectra of as-deposited $(GeSe_2)_{100-x}(Sb_2Se_3)_x$ thin films are given in Fig. 5. The dominant feature of the spectra is a broad band covering 130-230 cm^{-1} region similarly to Raman response of bulk $(GeSe_2)_{100-x}(Sb_2Se_3)_x$ glasses [5]. Based on our previous work, Raman spectra are studied as a sum of ten Gaussian bands peaking at ~138, 155, 170, 190, 200, 215, 240-250, 265, 280, and 285-300 cm^{-1}.

PLD $GeSe_2$ thin films are mainly composed of $[GeSe_{4/2}]$ tetrahedra linked by corners (A_1 symmetric stretching mode of corner sharing $GeSe_{4/2}$ tetrahedra peaking at ~200 cm^{-1}). Raman band with maximum at ~215 cm^{-1} reveals the existence of edge shared Ge-based tetrahedra. Raman band peaking at ~170 cm^{-1}, along with a small contribution at ~270 cm^{-1}, identifies Ge-Ge homopolar bonds (in detail, $Ge_2Se_{6/2}$ and Ge-Ge_mSe_{4-m} (m = 1,2,3,4) entities). Broad Raman active vibrations with low intensity cover the ~230-320 cm^{-1} range and are mainly due to presence of homopolar Se-Se bonds from Se chains and rings.

Considering Ge-Sb-Se PLD films, two Raman bands are observed at ~200 and 215 cm^{-1} which, as in case of $GeSe_2$ films and as observed in bulk Ge-Sb-Se glasses, are attributed to A_1 symmetric stretching mode of corner linked $[GeSe_{4/2}]$ tetrahedra and to A_1^c breathing vibration mode of $[Ge_2Se_{8/2}]$ bi-tetrahedra connected by edges [5]. As expected, intensities of these two bands decrease when increasing Sb_2Se_3 content. The intensity ratio between corner-shared (CS) and edge-shared (ES) tetrahedra decreases when x increases leading to the conclusion that introduction of antimony will first break CS tetrahedra bonds. A broad, low intensity band is present in the region of ~230-330 cm^{-1}, which corresponds to homopolar Se-Se bonds possibly present in different entities (Se chains at ~235 cm^{-1}, $[GeSe_{4/2}]$ corner linked dimers at ~280 cm^{-1}). Raman features contributing at highest frequencies (i.e. ~300 cm^{-1}) can be attributed to F_2 asymmetric vibration mode of $GeSe_4$ tetrahedra [5]; this band tends to disappear at high antimony content.

The Raman spectra of Ge-Sb-Se PLD films differs strongly from bulk glasses due to the presence of an intense and broad band covering the ~160-230 cm^{-1} spectral range. When increasing antimony content, this band increases in intensity. Raman bands at ~170 cm^{-1} and ~270 cm^{-1} (Ge-Ge homopolar bonds) decrease with increasing content of antimony. On the contrary, Raman band with maximum at ~190 cm^{-1}, corresponding to Sb-Se bond stretching mode in $SbSe_{3/2}$ pyramids, appears for $(GeSe_2)_{100-x}(Sb_2Se_3)_x$ films when $x \geq 5$. Its intensity logically increases when x rises, as the network slowly evolves from tetrahedra dominated to a pyramidal one. Raman band assigned to homopolar Sb-Sb bonds is located at ~155 cm^{-1}. Intensity of this Raman feature, really weak in case of low Sb_2Se_3 content, increases with

#234197 - $15.00 USD Received 6 Feb 2015; revised 7 Mar 2015; accepted 7 Mar 2015; published 13 Mar 2015

increasing x in studied $(GeSe_2)_{100-x}(Sb_2Se_3)_x$ thin films. For thin films with x>50, the Raman spectra are dominated by the two bands at ~155 and 190 cm^{-1}.

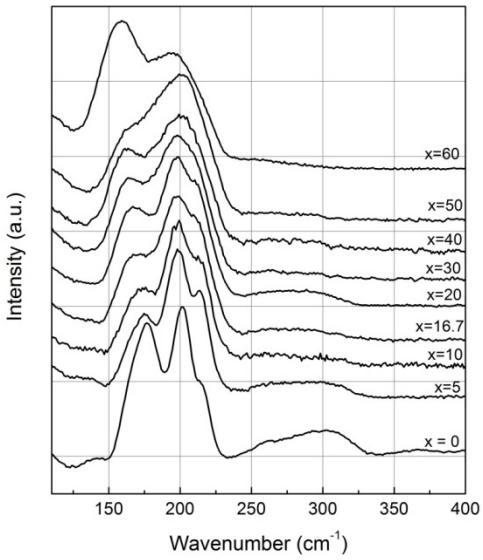

Fig. 5. Raman scattering spectra of PLD $(GeSe_2)_{100-x}(Sb_2Se_3)_x$ as-deposited thin films.

Differences between the global shape of Raman spectra of Ge-Sb-Se bulk glasses and as-deposited thin films are observed. It can be expected that proportions of individual structural entities are not the same. In order to determine structural changes occurring between bulk and thin films samples, differences between intensity ratios of main Raman features can be compared.

Then, four remarks regarding the differences between bulk and thin film structure can be done. (1) The main difference appears in ~150-190 cm^{-1} region. A strong increase of Raman intensity in this range is observed in case of thin films. (2) The ratio between Raman intensities attributed to Sb-Se bonds vibrations (190 cm^{-1}) and $GeSe_{4/2}$ tetrahedra modes (both CS and ES) is identical for bulk and thin films. (3) The ratio between Raman bands from homopolar Ge-Ge bonds (~170 cm^{-1}) and [$GeSe_{4/2}$] tetrahedra (ES and CS) modes is higher in case of thin films. (4) In thin films, homopolar Sb-Sb bonds are favored compared to [$SbSe_{3/2}$] entities.

The change of measured Raman spectra in ~150-190 cm^{-1} region can be attributed to the increase of number of Sb-Sb (~155 cm^{-1}) and Ge-Ge bonds ($Ge_2Se_{6/2}$ entities at ~170 cm^{-1}) in case of thin films, rather than to the increase of Sb-Se bonds contribution (~190 cm^{-1}). Thin films thus contain larger amount of [$Ge_2Se_{6/2}$] entities [30,37] and higher amount of homopolar Sb-Sb bonds when compared to the structure of bulk glasses. As shown in Table 1, chemical composition of thin films is slightly different from parent glasses, with some loss of Se which should be also taken into account to explain previous observations.

A comparison of Raman spectra of as-deposited and annealed thin Ge-Sb-Se films was done [Fig. 6]. Concerning $(GeSe_2)_{100-x}(Sb_2Se_3)_x$ thin films with low Sb_2Se_3 content (x<20), annealing induces a structural change, favoring corner-sharing tetrahedra in comparison with edge-sharing ones. Furthermore, in 150-190 cm^{-1} range, heteropolar Sb-Se bonds contribution decreases (intensity of the band peaking at ~190 cm^{-1} is lowered) whereas number of homopolar Sb-Sb, Ge-Ge, and Se-Se bonds increases (Raman bands at ~155, ~170 and ~265 cm^{-1}). This behavior is rather unusual as annealing process can induce a relaxation towards bulk structure [36,38] and often tends to reduce number of homopolar bonds [7,39].

#234197 - $15.00 USD Received 6 Feb 2015; revised 7 Mar 2015; accepted 7 Mar 2015; published 13 Mar 2015

The films with $(GeSe_2)_{80}(Sb_2Se_3)_{20}$ composition could be considered as an intermediate state where no structural changes can be observed after annealing and/or irradiation [Fig. 6(b)]. In Ge-Sb-Se thin films with higher Sb_2Se_3 content (x>20), annealing seems to induce a slight decrease in homopolar Sb-Sb and Ge-Ge bonds Raman response. Furthermore, no significant structural changes are observed between non irradiated and irradiated samples when x≤20. For x≥30%, irradiation seems to lead to a slight decrease of number of homopolar Sb-Sb and Ge-Ge bonds, depending on irradiation wavelength.

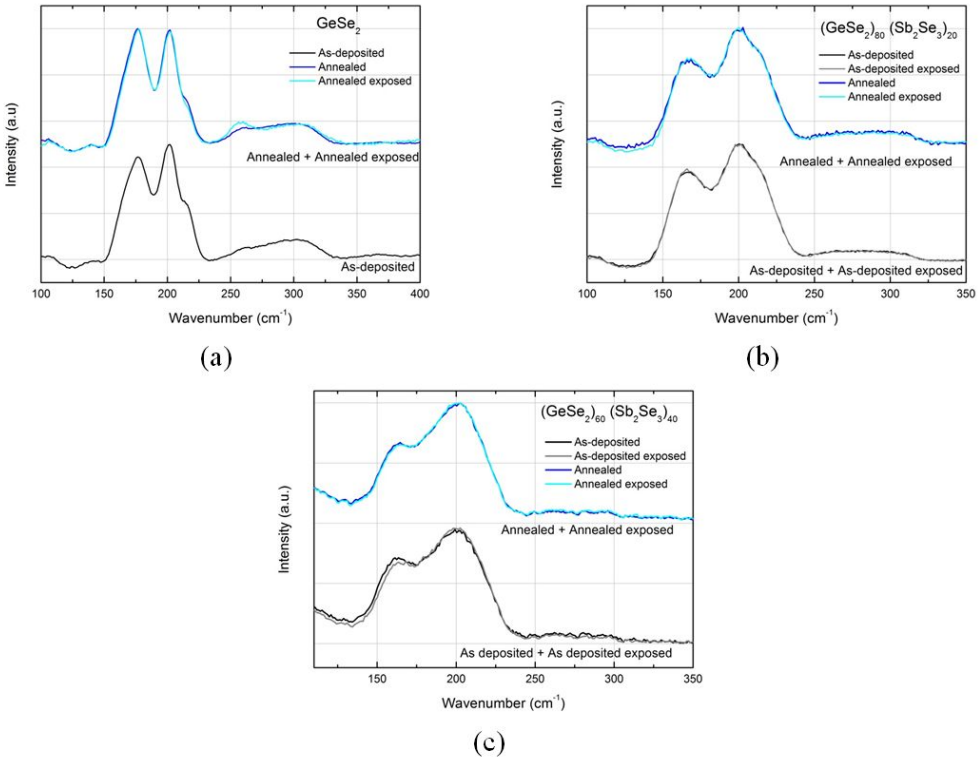

Fig. 6. Examples of Raman scattering spectra of $(GeSe_2)_{100-x}(Sb_2Se_3)_x$ thin films in different states (as-deposited, irradiated, annealed and irradiated after annealing): $GeSe_2$ (a), $(GeSe_2)_{80}(Sb_2Se_3)_{20}$ (b), and $(GeSe_2)_{60}(Sb_2Se_3)_{40}$ (c).

4. Conclusion

In this paper, $(GeSe_2)_{100-x}(Sb_2Se_3)_x$ amorphous chalcogenide thin film, deposited using pulsed laser deposition were studied in terms of photosensitivity/photostability (under irradiation with close to band gap light) and structure. The chemical composition of thin film was found to be in good agreement with glassy targets, despite a slight loss of selenium. The morphology study of fabricated films revealed neither cracks nor breaks; surface roughness was satisfactorily low. It was revealed that annealing tend to relax films' properties (refractive index and band gap) toward bulk glasses ones. Nevertheless, higher is the antimony concentration lower is the effect of annealing on optical properties.

After irradiation of as-deposited thin films in linear regime, a photobleaching effect is observed. Intensity of this phenomenon seemed to decrease when increasing antimony content. Irradiation of annealed films in linear regime induces a photodarkening effect in case of low Sb_2Se_3 content. When x≥30, photodarkening is not observed anymore and annealed films seem to be photostable. In nonlinear regime, highest photostability was observed for two pairs of films composition with x = 10, 16.7 and x = 30, 40. To conclude, when taking

#234197 - $15.00 USD Received 6 Feb 2015; revised 7 Mar 2015; accepted 7 Mar 2015; published 13 Mar 2015

into account photosensitivity/photostability in both, linear and nonlinear regime, the highest photostability (evaluating best possible combination of all parameters of interest described in this work, i.e. lowest possible change of E_g^{opt}, lowest possible change of refractive index and highest possible I_{0T} values*)* was indicated for layers with x = 30 and 40; such films seem to be suitable for nonlinear applications. Appearance of "compositional threshold" in $(GeSe_2)_{100-x}(Sb_2Se_3)_x$ pseudo-binary system at x = 40 proposed by Tichy *et al.* [40] using simple covalent bonds statistics in chemically ordered network model supports our conclusion regarding photostability around x = 40.

Finally, Raman scattering spectroscopy data were analyzed in order to understand the structure of the films and its change due to annealing/irradiation. To complete and confirm observed phenomena, a kinetic study of photosensitivity will be performed in near future.

Acknowledgments

Czech Science Foundation (Project No. 15-02634S), Ministry of Education, Youth, and Sports of the Czech Republic (Project CZ.1.07/2.3.00/30.0058 "Development of Research Teams at the University of Pardubice") and CNRS (PICS-CAPLA) financially supported this work.

#234197 - $15.00 USD Received 6 Feb 2015; revised 7 Mar 2015; accepted 7 Mar 2015; published 13 Mar 2015